Int. J. Appl. Math. Comput. Sci., 2004, Vol. 14, No. 2, 139–147

DYNAMIC STABILITY AND SPATIAL HETEROGENEITY IN THE INDIVIDUAL-BASED MODELLING OF A LOTKA-VOLTERRA GAS

JACEK WANIEWSKI[*,**], WOJCIECH JĘDRUCH[***], NORBERT S. ŻOŁEK[*]

[*] Institute of Biocybernetics and Biomedical Engineering, Polish Academy of Sciences
ul. Trojdena 4, 02–109 Warsaw, Poland
e-mail: {jacekwan, norbert}@ibib.waw.pl

[**] Interdisciplinary Centre for Mathematical and Computational Modelling
Warsaw University, ul. Pawińskiego 5A, 02–106 Warsaw, Poland
e-mail: jacekwan@icm.edu.pl

[***] Faculty of Electronics, Telecommunications and Informatics
Technical University of Gdańsk
ul. Narutowicza 11/12, 80-952 Gdańsk, Poland
e-mail: wjed@pg.gda.pl

Computer simulation of a few thousands of particles moving (approximately) according to the energy and momentum conservation laws on a tessellation of 800×800 squares in discrete time steps and interacting according to the predator-prey scheme is analyzed. The population dynamics are described by the basic Lotka-Volterra interactions (multiplication of preys, predation and multiplication of predators, death of predators), but the spatial effects result in differences between the system evolution and the mathematical description by the Lotka-Volterra equations. The spatial patterns were evaluated using entropy and a cross correlation coefficient for the spatial distribution of both populations. In some simulations the system oscillated with variable amplitude but rather stable period, but the particle distribution departed from the (quasi) homogeneous state and did not return to it. The distribution entropy oscillated in the same rhythm as the population, but its value was smaller than in the initial homogeneous state. The cross correlation coefficient oscillated between positive and negative values. Its average value depended on the space scale applied for its evaluation with the negative values on the small scale (separation of preys from predators) and the positive values on the large scale (aggregation of both populations). The stability of such oscillation patterns was based on a balance of the population parameters and particle mobility. The increased mobility (particle mixing) resulted in unstable oscillations with high amplitude, sustained homogeneity of the particle distribution, and final extinction of one or both populations.

Keywords: predator-prey system, entropy, correlation coefficient

1. Introduction

Individual-based simulations of population systems (e.g. using cellular automata and particle modelling methods) may yield counter-intuitive results when compared with the standard approach to population dynamics using ODEs or PDEs (Durrett and Levin, 1994). In fact, individual-based methods operate in an intermediate regime, where the number of individuals is rather low, their size cannot be neglected, and their movement is limited in space and velocity. Several studies on individual-based models of the simple Lotka-Volterra system of prey-predator interactions have shown a spatial instability of the system and dynamic spatio-temporal patterns arising out of an initially (quasi) uniform distribution of individuals (Boccara *et al.*, 1994; 1998; Lipowski, 1999; Lipowski and Lipowska, 2000; Satulovsky, 1996; Satulovsky and Tome, 1994; 1997; Tainaka and Fukazawa, 1992; Waniewski and Jędruch, 2000; Wilson *et al.*, 1995; 1993), and this observation was in contradiction to the theoretical description of the system by reaction-diffusion equations. The simplicity of the Lotka-Volterra equations needs a caricature description of biological interactions between individuals in computer simulations. They are reduced to a constant probability of prey multiplication (density independent with exponential growth of prey population, or allowed only if there is an empty space in the prey vicinity with a logistic type of the prey popula-

tion growth), constant probability of predator death, and an immediate exchange of the caught prey with a new predator (Boccara *et al.*, 1994; 1998; Lipowski, 1999; Lipowski and Lipowska, 2000; Satulovsky, 1996; Satulovsky and Tome, 1994; 1997; Tainaka and Fukazawa, 1992; Waniewski and Jędruch, 2000; Wilson *et al.*, 1995; 1993).

Individual-based simulations were applied also to more realistic and more sophisticated biological systems. The type II predator functional response (modelled as a time lag between catching a prey and the multiplication of the catcher) was studied by MacCauley, De Roos and Wilson in a series of papers (McCauley *et al.*, 1993; 1996; Roos *et al.*, 1991; 1998). These simulations involved three populations, with satiated predators being the third one. A further complication in the simulations involved a population of young predators, which cannot multiply and have a lower mortality than adults (McCauley *et al.*, 1993; 1996). Rand, Keeling and Wilson discussed individual-based simulations of a three-population system (resource, prey, predator) that, in the mean field approximation, reveals chaotic behaviour (Rand, 1994; Rand *et al.*, 1995; Rand and Wilson, 1995). In all those studies a departure of the spatial distribution of individuals from an initially homogenous one was found.

The patchiness of particle distribution in those studies was documented mostly by figures presenting the distribution of particles on the grid at a few selected moments of the system time evolution (Boccara *et al.*, 1994; 1998; McCauley *et al.*, 1993; 1996; Rand, 1994; Rand *et al.*, 1995; Rand and Wilson, 1995; Satulovsky, 1996; Satulovsky and Tome, 1994; 1997; Tainaka and Fukazawa, 1992; Waniewski and Jędruch, 2000; Wilson *et al.*, 1995; 1993). In the present study we propose a method for quantitative assessment of the departure from homogeneous distribution and the evaluation of the non-homogeneity of the distribution using the distribution entropy and correlation coefficient for the distributions of two populations. Furthermore, we evaluate the consequences of pattern formation for time evolution of the population system.

2. Computer Model of a Lotka-Volterra Gas

A short description of our simulation model is provided below. More details can be found in (Waniewski and Jędruch, 2000). Particles move on a tessellation of 800×800 squares according to a discrete clock. Each site may be occupied by no more than one particle. Periodic boundary conditions are applied. Between collisions the particles move (on the average) with a prescribed velocity vector $\mathbf{v} \in \mathbb{R}^2$ along approximately straight lines with the direction defined by vector $\mathbf{v}$. The motion is performed by jumping twice to one of the actual four neighbour squares (two neighbours in vertical and two in horizontal directions) with the probabilities adjusted to the components of $\mathbf{v}$. The direction of particle movement and its displacement after many time steps resembles a trajectory of free motion with a constant velocity along a straight line. The above rules impose maximum particle displacement per unit time step. It consists in one jump per time step if the velocity vector is horizontal or vertical. A collision occures if particles are in two adjacent squares (i.e. the squares with a common edge). During the collision, the particles change their velocities according to the law of scattering of two elastic discs; the law includes, however, a random factor that reflects an uncertainty caused by the discretization of disc movement on the tessellation. This rule was not efficient for collisions of more than two particles, i.e. if clusters of three or more particles were formed. Clusters are defined here as particles which are in contact through the edges of their cells. The rule for the movement of particles forming such clusters was based on the well-known phenomenon of elastic scattering in one dimension: if a ball hits a row of a few standing balls, then it stops and the ball on the other end of the raw starts to move with the same velocity as the hitting ball. Thus, in our simulations the horizontal components of velocities of particles forming a continuous raw are redistributed in increasing order from the left to the right. Then, the magnitude of the horizontal velocity is selected at random and all particles with the absolute value of the horizontal velocity are moved according to the direction of their horizontal velocities as one block. In this way the raw may be split into three parts: the left part moves one cell to the left, the middle one remains in place, and the right one moves one cell to the right. The process of splitting is, however, random and depends on the distribution of velocities in the raw. In an analogous way the particles forming a column are moved. Generally, this rule defines the tendency of particles to avoid staying in clusters, but rather to break the cluster into smaller ones.

There are two types of particles: the prey (U) and the predator (V). During a collision of U and V, U is changed into V with probability α_C per collision; the velocity of the new V particle is the same as the velocity of the U particle. This procedure may be interpreted as an act of predation and immediate multiplication of the predator; it is, however, more similar to a chemical reaction than to biological interactions. Each prey may give birth to a new prey with probability α_U per time step; the new prey is located in the vicinity of the "mother" prey according to a probability distribution over the particle neighbour cells, which is a decreasing function of the distance from the particle. If the selected square is occupied, then a new one is searched. In this way the effect of crowding on prey multiplication is avoided. Each predator may die with probability α_V per time step. With spatial

effects neglected, the equations for the rate of the change of the size of the populations (or their local density) would be the standard Lotka-Volterra equations:

$$\begin{cases} \dfrac{\mathrm{d}U}{\mathrm{d}t} = \alpha_U U - \beta UV, \\ \dfrac{\mathrm{d}V}{\mathrm{d}t} = -\alpha_V V + \beta UV, \end{cases} \tag{1}$$

where β depends on α_C and the mobility of particles.

Updating the system state is asynchronous with the random order of particle selection for updating. The movement of all particles is realized before the changes in the size of the populations (birth, death, predation). Initially all particles have the same absolute velocity and a randomly selected direction of the velocity. However, after 300 preparatory times steps of system evolution without any change in the number and type of particles, the distribution of the absolute values of velocities changes into an equilibrium (Maxwell-like) one. The newly born U particles have the initial (the same for all particles) absolute value of the velocity and a randomly chosen velocity direction.

3. Entropy and Correlation Coefficient for Spatial Distribution of Populations

A coarse-grained structure is imposed on the tessellation with grains of the typical size of 50×50 squares (c.f. (Poland, 1989; Rand, 1994; Rand *et al.*, 1995) for another application of the coarse-grained space for the analysis of individual-based simulations). Then the density of the particle distribution may be defined as a function of the grain position:

$$\rho_i = \frac{\text{number of particles in the } i\text{-th grain}}{\text{total number of particles}}. \tag{2}$$

The entropy of the distribution is defined in relation to the grain structure of the tessellation as follows:

$$\mathrm{Ent} = -\sum_{i \in \text{grains}} \rho_i \ln(\rho_i). \tag{3}$$

Furthermore, normalized entropy, $N\,\mathrm{Ent}$, is defined as $N\,\mathrm{Ent} = \mathrm{Ent}/\mathrm{Ent}_{\max}$, where $\mathrm{Ent}_{max} = \ln$ (number of grains) is the maximal possible value of entropy for a given grain structure (note that $\rho_i = 1/(\text{number of grains}) = \overline{\rho}$ for uniform distribution of particles between grains, cf. (3)). Thus $0 \le N\,\mathrm{Ent} \le 1$. However, for a low number of particles placed randomly on the tessalation (in this way we realized quasi-uniform distribution of particles on the tessalation), the normalized entropy is lower than one, depends on the number of particles, and approaches one only for a sufficiently high number of particles (Fig. 1). To correct this effect, we normalized $N\,\mathrm{Ent}$ once more for an empirically found maximal practical value of $N\,\mathrm{Ent}_{\max}$ for the given number of particles N. We found that within the range of the N values that appear in our simulations, we have

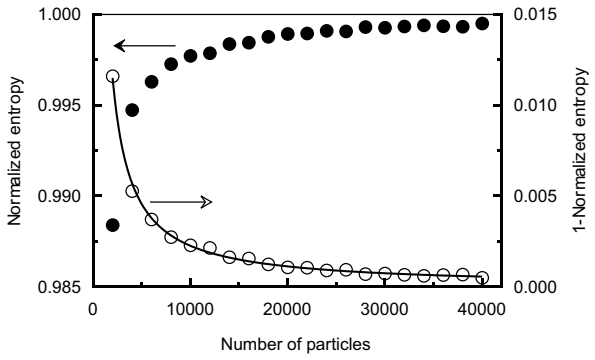

Fig. 1. Normalized (non-scaled) entropy (filled circles) as a function of the number of particles and the scaling of the normalized entropy for its values for small numbers of particles. Continuous line: the best fit to experimental points (open circles) of the function $1 - N\,\mathrm{Ent}_{\max} = 25.5$ (Number of particles)$^{-1.013}$. Tessellation size 800×800, grain size 50×50.

$$N\,\mathrm{Ent}_{\max} \approx 1 - aN^b,$$

where a and b were found for each specific tessalation size separately by a random distribution of different numbers of particles and calculations of $N\,\mathrm{Ent}_{\max}$ for various sizes of grains, see Fig. 1 for an example of such calculations.

The cross-correlation coefficient, R_{UV}, between the distributions of U and V particles was calculated using

$$R_{UV} = \frac{\sum_{i \in \text{grains}} (\rho_{Ui} - \overline{\rho})(\rho_{Vi} - \overline{\rho})}{\sqrt{\sum_{i \in \text{grains}} (\rho_{Ui} - \overline{\rho})^2} \sqrt{\sum_{i \in \text{grains}} (\rho_{Vi} - \overline{\rho})^2}},$$

where $\overline{\rho} = 1/(\text{number of grains})$ denotes the density of the uniform distribution of particles.

The tendency of particles for clustering was also recorded in a more direct way by counting the number of clusters and the number of particles (for each particle type separately) in clusters. Three types of clusters were defined: Type I — tight clusters with an edge-to-edge neighborhood, Type II — tight clusters with an edge-to-edge and corner-to-corner neighbourhood, and Type III — loose clusters with a neighbourhood containing all cells at a distance less than two cells in horizontal or vertical directions, cf. Fig. 2 for examples of different types of clusters.

Table 1. Characteristics of computer simulations calculated for one oscillation period (except entropy) defined as the time interval between consecutive maxima of the amount of U particles, mean $\pm$ SD.

	A (8000/8000)$^{f)}$	A1 (13500/13500)$^{f)}$	A2 (5000/5000)$^{f)}$	B (8000/8000)$^{f)}$
Density $U^{a)}$	213±5	214±6	215±4	52±4
Density $V^{a)}$	211±5	210±4	211±5	53±5
Cycle period	554±74	585±116	568±66	1928±247
$\varphi^{b)}$	0.187±0.069	0.186±0.068	0.199±0.091	0.165±0.038
Maximum / Average $U^{c)}$	1.383±0.206	1.321±0.124	1.350±0.158	2.226±0.741
Maximum U/Maximum $V^{d)}$	1.025±0.141	1.009±0.153	1.018±0.161	1.074±0.093
Entropy $U^{e)}$	0.911±0.019	0.911±0.013	0.912±0.015	0.944±0.006
Entropy $V^{e)}$	0.929±0.015	0.928±0.01	0.929±0.011	0.963±0.004

$^{a)}$ amount of particles per unit size area of 100×100 squares
$^{b)}$ phase shift between a maximum of the V amount and the preceding maximum of the U amount
$^{c)}$ ratio of maximal over average amount of U particles
$^{d)}$ ratio of a maximum of the U amount over the consecutive maximum of the V amount
$^{e)}$ entropy of the spatial particle distribution calculated from 5000 to 30,000 time steps
$^{f)}$ initial numbers of U and V (U/V)

4. Results

Two simulations of the system with various parameters for the populations were examined. Simulation A had more vigorous dynamics of the multiplication of U ($\alpha_U = 0.016$) and the death of V ($\alpha_V = 0.016$), more frequent interactions between U and V ($\alpha_C = 1$), and a higher density of particles, whereas the population dynamics in Simulation B were more moderate ($\alpha_U = \alpha_V = 0.004$, $\alpha_C = 1$), see Table 1 and Figures 3 and 4. The initial velocity of particles was one in both simulations (with the limit velocity equal to five, c.f. (Waniewski and Jedruch, 2000)). Two additional simulations, A1 and A2 (Table 1), with the same parameters as in Simulation A but with a different initial number of particles, were also included into the study. All simulations were carried out for 30,000 time steps. The studied variables were recorded every 10 time steps.

In Simulations A and B we observed sustained oscillations with a variable amplitude (Figs. 3 and 4). The normalized entropy decreased from the value close to one in the initial state of the system and oscillated in the same rhythm as the populations (Figs. 3–5). The entropy of the distribution of U was smaller than the distribution entropy of V. This reflects a higher tendency of U to cluster due to their multiplication. In both simulations the distribution entropy never returned back to the initial value of one, i.e. the distribution of particles remained nonhomogeneous after the departure from the initial (quasi) homogeneous distribution. The oscillations of the entropy in phase with oscillations of the population, i.e. the decrease in entropy with the decrease in the population size, showed that during the oscillations the spatial distribution of the population was more 'patchy' (as measured by the entropy) than for the population with more individuals which have to be spread over a larger area. The patchiness of the particle distribution was higher in Simulation A than in Simulation B, as demonstrated by the values of the average normalized entropy (Table 1).

The normalized entropy depended on the size of grains used for its evaluation (Fig. 6). However, the qualitative features of the time-pattern of the entropy were almost independent of the grain size, especially for grains of smaller sizes (less than 100, Fig. 6). The oscillations of the cross-correlation coefficient were more irregular and had a tendency for a frequency twice as high as the oscillations of the entropy and the amount of particles for one population (Fig. 7), which reflected the shift in phase

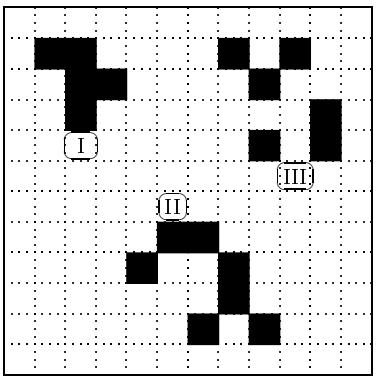

Fig. 2. Examples of clusters of different types.

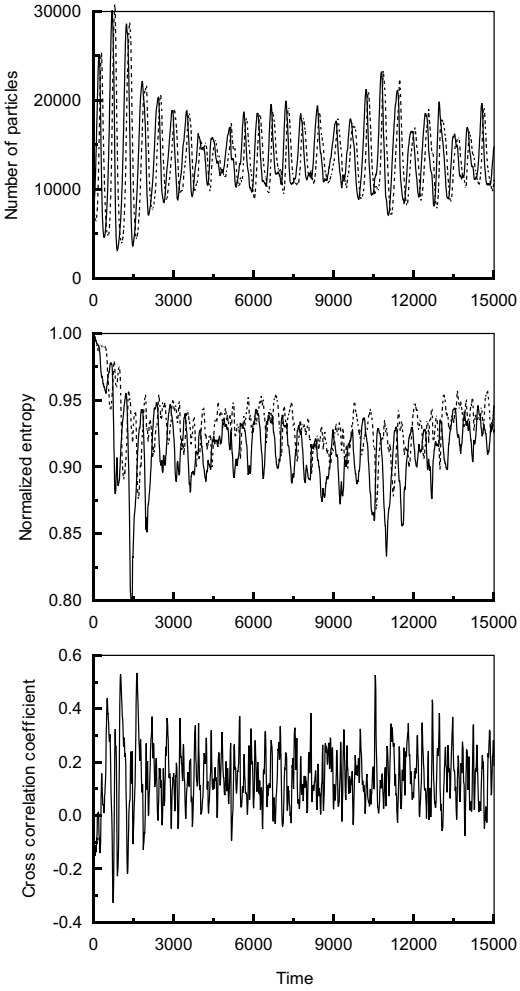

Fig. 3. Time evolution of the number of the U and V particles (top panel; continuous line – particles U, dashed lines – particles V), normalized entropy of the U and V space distributions (middle panel; continuous line – particles U, dashed lines – particles V), and cross correlation coefficient R_{UV} (bottom panel), shown for initial 15,000 time steps of Simulation A. The normalized entropies and cross correlation coefficient were evaluated for 50×50 grains.

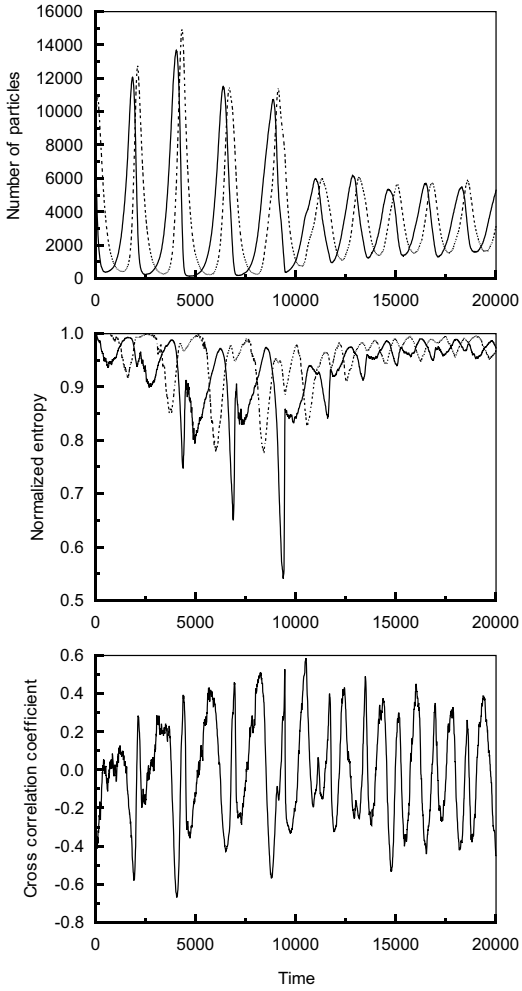

Fig. 4. Time evolution of the number of the U and V particles (top panel; continuous line – particles U, dashed lines – particles V), normalized entropy of the U and V space distributions (middle panel; continuous line – particles U, dashed lines – particles V), and cross correlation coefficient R_{UV} (bottom panel) shown for initial 20,000 time steps of Simulation B. The normalized entropies and cross correlation coefficient were evaluated for 50×50 grains.

between the U and V oscillations. The momentary, as well as time average values of the cross-correlation R_{UV} also depended on the size of the grain (Fig. 7). Note that the time-average cross-correlation coefficient changes from negative values for small grain sizes to positive ones for larger grain sizes. The negative values of R_{UV} imply the separation of U and V populations in space. The tendency of the populations to separate in space had a higher space scale for moderate dynamics (Simulation B) than for fast dynamics (Simulation A).

Clusters appeared more often and were larger in Simulation A than in Simulation B. A more detailed description of clusters of Type I, II, and III in Simulation A is given in Table 2. Clusters of Type I reached occasionally the size of 700–800 particles and on the average about 13% of particles were in those clusters. Most of the clusters had from 3 to 9 particles, as follows from the comparison of the total number of clusters and the number of large (more than 9 particles) clusters in Table 2. Furthermore, over 60% of particles were concentrated in the loose clusters of Type III. Particles U had a stronger tendency to aggregate than particles V, and this tendency was even more visible for large clusters. The respective values in Simulation B were 10–100 times lower (data not shown).

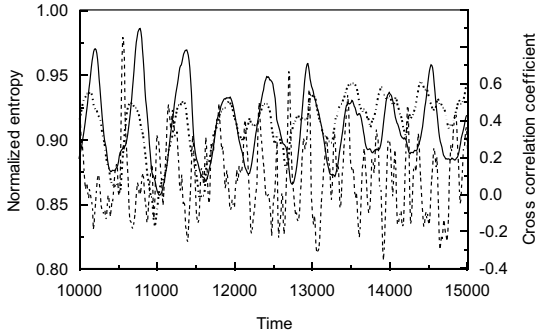

Fig. 5. Normalized entropy of the distribution of U particles (dotted line), cross correlation coefficient R_{UV} (dashed line), and the number of U particles (continuous line, scale not shown) versus time for a selected time interval of Simulation A.

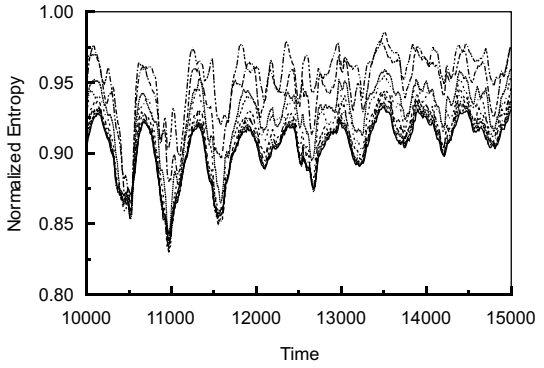

Fig. 6. Normalized entropy of U particles calculated for various sizes of grains versus time for a selected time interval of Simulation A. Grain sizes: 16×16, 20×20, 25×25, 32×32, 40×40, 50×50, 80×80, 100×100, 160×160, 200×200. The value of entropy increases with the increased grain size.

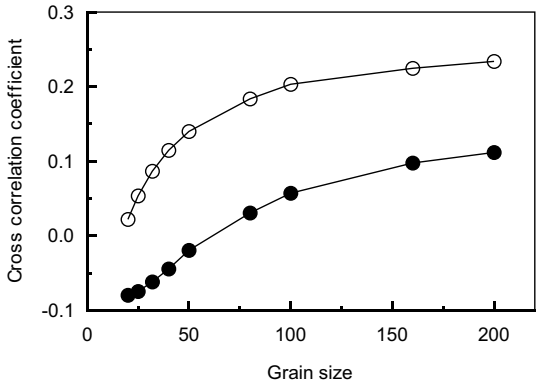

Fig. 7. Time average (from 5000 to 30,000 time steps) of the cross-correlation coefficient R_{UV} as a function of the grain size for Simulations A (open circles) and B (closed circles). Grain sizes as in Fig. 6.

The time-average characteristics of the number of particles did not differ between simulations with the same parameters but different initial numbers of the particles as demonstrated in Simulations A, A1 and A2 (Fig. 8 and Table 1). This observation is in contrast to the well-known feature of Lotka-Volterra equations (which were the basis for the arrangements of the interaction in our individual-based model of the system) stating that the amplitude of the oscillations of the populations size depends on the initial conditions.

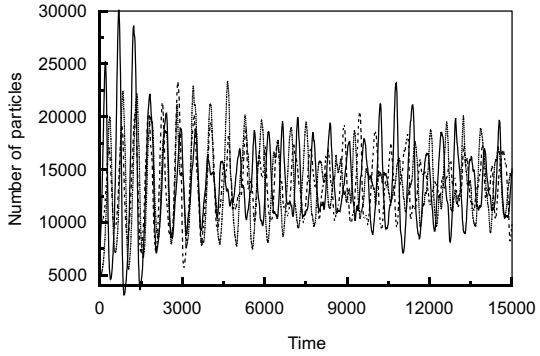

Fig. 8. Time evolution of the number of U particles for Simulations A (continuous line), A1 (dashed line) and A2 (dotted line) during the initial 15,000 time steps. Description of the simulations in the text and Table 1.

The dynamic spatio-temporal patterns yielded the low and oscillating entropy of particle distribution and the cross correlation coefficient R_{UV} that oscillated between negative and positive values (Figs. 3 and 4). The patterns resulted from the adjustment between the local dynamics of the populations and the mobility of the particles, and contributed to the stability system. An example of the importance of this adjustment was demonstrated in Simulation B1 (Fig. 9). There, the initial state of

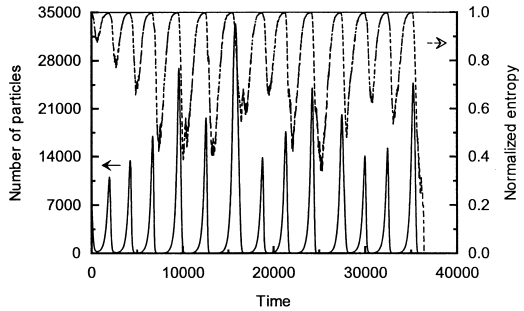

Fig. 9. Time course of the number of U particles and normalized (but not scaled) entropy for U distribution in simulation B1. The initial state of the system as in Simulation B; velocity of newborn U particles was equal to five; the probability of the interaction of U and V during a collision was equal to 0.35; other parameters as in simulation B.

Table 2. Statistics of clusters in Simulation A.

	Number of clusters [c)]	Fraction of particles in clusters (%) [d)]	Fraction of U particles in clustered particles (%) [e)]
All clusters [a)]			
Type I	963±324	13±2	61±8
Type II	1618±455	26±5	60±8
Type III	2115±332	61±6	55±7
Large clusters [b)]			
Type I	13±13	< 1	74±20
Type II	64±38	4±2	70±12
Type III	252±67	31±7	60±8

[a)] clusters with three or more particles,
[b)] clusters with ten or more particles,
[c)] average number of clusters per one time step (mean ± SD),
[d)] ratio of the amount of particles in clusters over the total number of particles per one time step (mean ± SD),
[e)] ratio of the amount of U particles in clusters over the amount of all particles in clusters (mean ± SD).

the particles was identical as in Simulation B. However, the newborn U particles had a higher mobility ($v = 5$, i.e. the maximal possible displacement per one time step, in contrast to $v = 1$ in Simulation B), and soon the average mobility of the particles was much higher than in Simulation B. To keep the average number of particles at a level similar as in Simulation B, we decreased the probability of the interaction between the U and V particles to 0.35 (from 1 in Simulation B). Therefore the probability of the death of a U particle and the birth of a V particle, which was equal to the probability of the collisions between U and V multiplied by the probability of the effective interaction during the collision was similar in both simulations. In spite of this adjustment, the system from Simulation B1 was unstable with the high amplitude of oscillations. After a few cycles, particles U got extinct (Fig. 9), and soon the population of V particles died out too. This kind of instability usually results in the extinction of one of the populations at the minimum of its number and is often observed for small numbers of particles in the system (Waniewski and Jędruch, 1999). Notice that in contrast to Simulation B, the normalized entropy during the whole simulation time was coming back to the maximal value when the number of particles was high (Fig. 9), which means that the distribution of particles was homogenous at these moments.

5. Discussion

The evolution of the Lotka-Volterra system in individual-based simulations differs in many respects from its descriptions by ODEs or reaction-diffusion PDEs. The dynamic spatio-temporal patterns, the drift of the oscillation phase between different sub-areas of the tessellation, and the independence of the oscillation amplitude of the initial conditions demonstrate these differences. Generally, it is well known that stochastic versions of some models (and individual-based models are mostly stochastic) may yield quite different predictions than those from their deterministic versions (Renshaw, 1991). Among other features that can make a difference between individual-based simulations and their simple mathematical models are nonlocality and a non-standard diffusion process (Waniewski and Jędruch, 2000).

On the other hand, the individual-based simulations of the system retain many features of the Lotka-Volterra model, as oscillations with a relatively stable period, a stable phase shift between the cycles of U and V, similar amplitudes of the U and V oscillations if the dynamic parameters for both populations are the same, oscillations similar to harmonic ones for a small amplitude and high thin peaks between wide troughs for high amplitudes, and similar average values of the population numbers for all cycles (Table 1). Furthermore, the parameters of Lotka-Volterra equations may be estimated with high accuracy, especially if an appropriate size of the observation window is selected (Waniewski and Jędruch, 1999; Waniewski and Jędruch, 2000).

The oscillations of the system in individual-based simulations are stable only for adequately selected parameters. The stability of the oscillations is related to the instability of the homogeneous distribution of particles and

the formation of their aggregates, i.e. to the decrease in the entropy of the particle distribution. However, the details of the particle motion do not seem to be important for those phenomena. In fact, similar results were obtained with gas-like mobility (in the present study), random walk (Wilson *et al.*, 1995), and for a stochastic gas lattice, i.e. without any particle motion (Satulovsky, 1996; Satulovsky and Tome, 1994; 1997; Tainaka and Fukazawa, 1992). In the last case it was possible to formulate a mathematical model of the system using the master equation and decoupling by a mean-field approximation. The pair approximation analysis demonstrated the instability of the homogeneous states (Satulovsky and Tome, 1997).

The importance of the clustering of U particles on the behaviour of the Lotka-Volterra system was analyzed in detail by Poland using ODEs and lattice models (Poland, 1989). He showed that the clustering of preys (U) yielded limit cycles, at least for some range of the parameters. This effect might indeed contribute to the observed features of the system trajectories in our simulation, although the intrinsic stochasticity of the model did not allow for the approach to a stable trajectory. Furthermore, both U and V formed clusters in the presented simulations (Table 2).

The temporal and spatial patterns of the interacting populations may be studied using various methods (Adami, 1998; McCauley *et al.*, 1996; Rand *et al.*, 1995; Ranta and Kaitala, 1997; Roos *et al.*, 1998; Satulovsky, 1996; Wiegand *et al.*, 1999). Most of them were applied to characterize a static landscape or averaged-over-time behaviour, or to determine a characteristic spatial scale of the system. In the current study, the entropy and cross-correlation coefficient of particle distribution and the analysis of the system and the model parameters using different observation windows were applied to follow the time evolution of the system and spatial distribution of populations. The other methods may also be used for this purpose, and the grained entropy and cross-correlation coefficient do not exhaust all possible ones. However, they are simple, may be easily applied to particle computer simulations, as well as to field and experimental studies, and should be considered as an alternative or complementary way to study spatial phenomena in simulated and real systems.

Complex spatio-temporal patterns have been recently reported for animal populations, which are known to be involved in predator-prey systems. A phase shift between oscillations and its irregular drift was reported for the Canadian lynx population in various Canadian provinces (Ranta *et al.*, 1997). Waves of vole population travelling through Finland and France are another example of such patterns (Ranta and Kaitala, 1997). Beside numerous (density dependent and independent) factors, which may affect any real population, spatially distributed predator-prey interactions between individuals may substantially contribute to those effects by dynamical enhancement of local fluctuations in the populations size, as demonstrated by individual-based modelling of the system.

References

Adami C. (1998): *Introduction to Artificial Life*. — New York: Springer.

Boccara N., Cheong K. and Oram M. (1994): *A probabilistic automata network epidemic model with births and deaths exhibiting cyclic behaviour*. — J. Phys. A: Math. Gen., Vol. 27, pp. 1585–1597.

Boccara N., Roblin O. and Roger M. (1994): *Automata network predator-prey model with pursuit and evasion*. — Phys. Rev. E 50, Vol. 50, No. 6, pp. 4531–4541.

McCauley E., Wilson W.G. and de Roos A.M. (1993): *Dynamics of age-structured and spatially structured predator-prey interactions: Individual-based models and population-level formulations*. — Am. Naturalist, Vol. 142, No. 3, pp. 412–442.

McCauley E., Wilson W.G. and de Roos A.M. (1996): *Dynamics of age-structured predator-prey populations in space: Asymmetrical effects of mobility in juvenile and adult predators*. — OIKOS, Vol. 76, pp. 485–497.

Durrett R. and Levin S. (1994): *The importance of being discrete (and spatial)*. — Theor. Popul. Biol., Vol. 46, pp. 363–394.

Lipowski A. (1999): *Oscillatory behavior in a lattice prey-predator system*. — Phys. Rev. ER 60, No. 5, pp. 5179–5184.

Lipowski A. and Lipowska D. (2000): *Nonequilibrium phase transition in a lattice prey-predator system*. — Physica A 276, pp. 456–464.

Poland D. (1989): *The effect of clustering on the Lotka-Volterra model*. — Physica D 35, pp. 148–166.

Rand D.A. (1994): *Measuring and characterizing spatial patterns, dynamics and chaos in spatially extended dynamical systems and ecologies*. — Phil. Trans. R. Soc. Lond. A 348, pp. 497–514.

Rand D.A., Keeling M. and Wilson H.B. (1995): *Invasion, stability and evolution to criticality in spatially extended, artificial host-pathogen ecologies*. — Proc. R. Soc. Lond. B 259, pp. 55–63.

Rand D.A. and Wilson H.B. (1995): *Using spatio-temporal chaos and intermediate scale determinism to quantify spatially extended ecosystems*. — Proc. R. Soc. Lond. B 259, pp. 111–117.

Ranta E. and Kaitala V. (1997): *Travelling waves in vole population dynamics*. — Nature 390, pp. 456.

Ranta E., Kaitala V. and Lundberg P. (1997): *The spatial dimension in population fluctuations*. — Science 278, pp. 1621–1623.

Renshaw E. (1991): *Modeling Biological Populations in Space and Time*. — Cambridge: Cambridge University Press.

De Roos A.M., McCauley E. and Wilson W.G. (1991): *Mobility versus density-limited predator-prey dynamics on different spatial scales*. — Proc. R. Soc. Lond. B 246, pp. 117–122.

De Roos A.M., McCauley E. and Wilson W.G. (1998): *Pattern formation and the spatial scale of interaction between predators and their prey*. — Theor. Popul. Biol. 53, No. 2, pp. 108–130.

Satulovsky J.E. (1996): *Lattice Lotka-Volterra models and negative cross-diffusion*. — J. Theor. Biol. 183, pp. 381–389.

Satulovsky J.E. and Tome T. (1994): *Stochastic lattice gas model for a predator-prey system*. — Phys. Rev. E 49, No. 6, pp. 5073–5079.

Satulovsky J.E. and Tome T. (1997): *Spatial instabilities and local oscillations in a lattice gas Lotka-Volterra model*. — J. Math. Biol. 35, pp. 344–358.

Tainaka K. and Fukazawa S. (1992): *Spatial pattern in a chemical reaction system: prey and predator in the position-fixed limit*. — J. Phys. Soc. Jpn. 61, No. 6, pp. 1891–1894.

Waniewski J. and Jędruch W. (1999): *Individual based modeling and parameter estimation for a Lotka-Volterra system*. — Math. Biosci. 157, pp. 23–36.

Waniewski J. and Jędruch W. (2000): *Spatial heterogenity and local oscillation phase drifts in individual-based simulations of a prey-predator system*. — Int. J. Appl. Math. Comp. Sci., Vol. 10, No. 1, pp. 175–192.

Wiegand T., Moloney K.A., Naves J. and Knauer F. (1999): *Finding the missing link between landscape structure and population dynamics: A spatially explicit perspective*. — Am. Nat., Vol. 154, No. 6, pp. 605–627.

Wilson W.G., McCauley E. and de Roos A.M. (1995): *Effect of dimensionality on Lotka-Volterra predator-prey dynamics: individual based simulation results*. — Bull. Math. Biol., 57, No. 4, pp. 507–526.

Wilson W.G., de Roos A.M. and McCauley E. (1993): *Spatial instabilities within the diffusive Lotka-Volterra system: Individual-based simulation results*. — Theor. Popul. Biol. 43, pp. 91–127.

Received: 18 March 2003
Revised: 10 October 2003
Re-revised: 6 March 2004